Order and Mobility in Polycarbonate−Poly(ethylene oxide) Blends Studied by Solid-State NMR and Other Techniques

J. Brus,* J. Dybal, P. Schmidt, J. Kratochvíl, and J. Baldrian

Institute of Macromolecular Chemistry, Academy of Sciences of the Czech Republic, 162 06 Prague 6, Czech Republic

Received March 27, 2000

ABSTRACT: Solid-state 1D and 2D ^{13}C CP/MAS NMR and ^{1}H CRAMPS (combined rotation and multipulse spectroscopy) and Raman spectroscopy, X-ray scattering, and DSC were used to investigate the structure, morphology, and dynamic behavior of blends of two semicrystalline polymers, polycarbonate (PC) and poly(ethylene oxide) (PEO). The splitting of aromatic carbon signals in the ^{13}C CP/MAS NMR spectra and the absence of spinning sidebands in the ^{1}H dipolar spectra (2D WISE) indicate restricted mobility and hindered cooperative motions of PC chains resulting from blending of PC with PEO and from fixed ordering due to partial crystallinity of PC itself. The observed multiple splittings of the signals of aromatic and carbonate carbons indicate comparable amounts of trans−trans and cis−trans conformational structures of the carbonate group. 2D WISE spectra prove large differences in molecular mobility of amorphous PEO and PC. High mobility of amorphous PEO is not imparted significantly to less mobile PC, despite intimate mixing in the amorphous phase of PC−PEO blends suggested by ^{13}C CP/MAS NMR spectra and CRAMPS $^{1}H-^{1}H$ homonuclear dipolar dephasing and proved by 2D CRAMPS and WISE spin diffusion measurements. The morphology and domain sizes at the nanometer scale were determined from analysis of spin diffusion processes.

Introduction

A lot of attention has been devoted in recent years to characterization of polymer blends. The increasing interest in polymer blends is mainly due to their importance in development of new materials with designed properties, which cannot be reached by using single polymers. Among various blends of our recent attention,[1−3] those based on two semicrystalline polymers, namely polycarbonate (PC) and poly(ethylene oxide) (PEO), are investigated in this paper. These blends show weak (van der Waals) interaction between the components leading to miscibility in the amorphous phase, and at the same time, both components can be crystalline. Generally, the microphase structure, the degree of phase separation of polymer blends, and molecular dynamics are research subjects of practical and scientific importance, because they determine mechanical and physical properties. In particular, their modification is interesting in our system containing glassy PC. It is known that macroscopic behavior of glassy polymers such as impact resistance and gas permeability are assumed to be associated with mid-kilohertz local motions of polymer chains. Phenyl 180° flip motions play an important role in β-relaxation of PC. This relaxation often disappears if the glass transition temperature is lowered by adding a plasticizer, the molecules of which apparently block the internal motions of the phenyl groups.[4] Although a lot of papers concerning the structure and dynamics of single PEO[2,5−7] and PC[5,8−14] as well as those dealing with various blends containing PEO[2,6,15] and/or PC[11,16,17] have been published, no work deals with the structure of PC−PEO blends. The studied material (PC−PEO blend) is a complex system consisting of two semicrystalline components. Besides crystallinity, miscibility, and molecular dynamics of both components in the blends, considerable attention in the present contribution has also been paid to the phase and supramolecular structure. To this end, several techniques of the solid-state ^{1}H and ^{13}C NMR spectroscopy have been used.

Various experimental techniques are available to study heterogeneity of these materials, e.g., IR, DSC, transmission electron microscopy, X-ray scattering, NMR spectroscopy. Because only a small number of polymer combinations lead to thermodynamically stable blends and the distinction between compatible and incompatible blends is in many cases not trivial, several one-dimensional and two-dimensional solid-state NMR techniques were proposed to study the level of mixing in polymer blends.[18] Detailed information about the molecular dynamics, morphology, miscibility, and domain size of polymer blends can be directly derived from NMR parameters such as dipolar dephasing, ^{1}H and ^{13}C line broadening, relaxation times, and spin diffusion. Of particular interest is the interaction between different components, especially in the interfacial region. A stronger interaction can result in greater modification of NMR spectrum relative to that of neat components (e.g., intermolecular hydrogen-bonding interaction can cause significant "downfield" shift).[6] These strong hydrogen-bonding interactions support mixing of systems such as poly(oxymethylene)−TPh (terphenphenol polymer composed of terpene and phenolic moieties)[6] or blends of PEO and poly(methyl methacrylate).[2,15] For a detailed understanding of mechanical properties, it is also essential to obtain information about the distribution of mobility in the material. There are various methods for qualitative characterization of molecular mobility, and among others, ^{1}H wide-line spectroscopy (WISE), where effective strength of dipolar couplings and thus molecular mobility are reflected, is well-known.[19] The desired information about the local dynamics for dynamically heterogeneous systems is provided by heteronuclear 2D WISE experiment.[19−23] Solid-state NMR also allows to study long-range ordered structures on the 0.5−500 nm scale via ^{1}H spin diffu-

10.1021/ma000533s CCC: $19.00
Published on Web 08/05/2000

sion.[19,22,24] So far, many systems have been studied by ^{1}H spin diffusion measurements, such as the polymer/additive system,[25] semicrystalline polymers,[26] polymer blends,[6,15,27] block copolymers,[24] copolyureas,[28] and biopolymers.[29]

Experimental Section

Materials. Samples were prepared from commercial-grade bisphenol A polycarbonate SINVET 251 (ENI, Italy) with a weight-average molecular weight (M_w) of 24 000 and a number-average molecular weight (M_n) of 9600, as measured by gel permeation chromatography, and from PEO ($M_w = 6 \times 10^5$) produced by BDH Chemicals, Ltd. (UK). DSC and WAXS measurements indicated lower crystallinity than 0.5% for the original PC samples. The samples of PC and PEO homopolymers and PC−PEO blends were obtained by dropwise precipitation from a chloroform solution (2% w/w) into pentane, slow evaporation of the solvents at room temperature, and subsequent heating in a vacuum oven at 85 °C for 1 h.

Calorimetric Measurements. DSC measurements were performed on a Perkin-Elmer Pyris 1 DSC apparatus cooled with liquid nitrogen and flushed with helium. The temperature scale was fitted with respect to the melting points of cyclohexane and indium; the power output scale was calibrated with indium. The as-prepared samples closed in aluminum pans were scanned in the temperature range from −20 to 280 °C at the heating rate 10 °C/min. In estimating the degree of crystallinity from the DSC data, the values of 131.9 and 196.6 J/g were used for the heats of fusion of 100% crystalline PC and PEO, respectively.[30]

Raman Measurements. Raman spectra were measured on a Bruker IFS-55 FT-IR spectrometer equipped with a Raman module FRA-106. Spectra were recorded at 2 cm^{-1} resolution and excited by a 1064 nm diode-pumped Nd:YAG laser with a power of 400 mW at a sample.

WAXS and SAXS. Wide-angle X-ray scattering (WAXS) patterns were obtained using a powder diffractometer HZG/4A of Freiberger Praezisionsmechanik GmbH (Germany). Cu Kα radiation was monochromatized with a Ni filter and pulse-height analyzer, and diffracted radiation was recorded by means of a proportional counter. The degree of crystallinity in semicrystalline samples of PC was calculated as the ratio of the integral intensity of the crystalline phase scattering to the total scattering intensity. The integral intensity corresponding to the crystalline phase was obtained after separation of the amorphous component by using the scattering of fully amorphous PC sample. Crystallinity of PEO in the blend was determined as the ratio of the integral intensity of the PEO crystalline reflections to the total intensity scattered by the PEO component. This value was obtained as a total intensity scattered by the mixture multiplied by known weight fraction of PEO in the mixture.

Small-angle X-ray scattering (SAXS) curves were measured using KRATKY system (A. Paar, Austria).). Cu Kα radiation was monochromatized with a Ni filter and pulse-height analyzer. Scattered intensity was registered by means of a position-sensitive detector.

NMR Measurements. NMR spectra were measured with a Bruker DSX 200 NMR spectrometer in 4 mm ZrO_2 rotor at the frequency 50.33 and 200.14 MHz (^{13}C and ^{1}H, respectively). The number of data points was 6K, magic angle spinning (MAS) frequency 3.2 kHz, and strength of B_1 field (^{1}H and ^{13}C) 62.5 kHz. The number of scans for accumulation of ^{13}C CP/MAS NMR spectra[31] was 3600, repetition delay of 4 s, and spin lock pulse of 0.7 ms. During detection, a high-power dipolar decoupling was used to eliminate strong heteronuclear dipolar coupling. ^{13}C scale was calibrated with glycine external standard (176.03 ppm, low-field carbonyl signal). Static and ^{1}H MAS NMR spectra were measured with the number of scans 32−256 and repetition delay of 10 s. The external standard HMDS (hexamethyldisiloxane) was used for calibration of the ^{1}H scale, its ^{1}H chemical shift being 0.05 ppm relative to TMS (tetramethylsilane). ^{1}H−^{1}H dipolar dephasing was studied using standard Hahn-echo pulse sequence ($\pi/2-\tau-\pi-\tau-$aq) with a variable τ value. The number of scans gradually increased with increasing dephasing time from 32 to 1024. For dipolar filter times larger than 1 ms the spectral width was reduced from 150 to 20 kHz, and the number of data points was increased to 32K to resolve narrow line (FID resolution was then 0.6 Hz per point). MAS frequency was 3.2−3.6 kHz. Static ^{1}H NMR spectra were measured by solid-echo pulse sequence ($\pi/2_x-\tau_1-\pi/2_y-\tau_2-$aq). Delays τ_1 and τ_2 were 8 and 3 μs, respectively, reflecting probe-head dead time.

2D WISE spectroscopy[19,20] employed 400 scans per one increment. The evolution period (t_1) between the ^{1}H 90° pulse and contact pulse consisted of 512 increments of 5 μs. Total t_1 FID resolution is then 400 Hz, which was sufficient to observe relatively narrow proton signals. The CP contact pulse was 0.7 ms to significantly minimize spin diffusion, and the repetition delay was 2 s.

The 2D WISE pulse sequence[21,22] with evolution time t_1 and spin diffusion mixing time τ_m was used to yield information about the domain size and morphology of the blends by means of spin diffusion. The mixing time varied from 0.1 to 50 ms; other parameters were the same as in standard WISE experiments described above. T_1 relaxation limits the maximum domain size, which can be determined by the proton spin diffusion experiment. For samples with a spatially constant relaxation time, its effect can be eliminated simply by an appropriate phase cycle of the pulses before the mixing time. Selected proton magnetization is now aligned along $-z$ and $+z$ axes in alternating scans. All signal contributions caused by T_1 relaxation are canceled.

For proton relaxation in rotating frame and cross-polarization dynamics measurement, we used standard spin-lock sequence with carbon detection and with varied duration of contact pulse from 0.1 to 20 ms.

In the 1D and 2D ^{1}H CRAMPS experiments, the BR-24 pulse sequence was used, with a 90° pulse length of 1.8 μs and the large and short delay of 3.8 and 1.0 μs, respectively. MAS was 2.5 kHz, data size of 2K points, and repetition delay of 4 s. The scaling and ^{1}H chemical shift were calibrated using aspartic acid. (The lowest field and the second high-field signals are 15.6 and 3.41 ppm, respectively.) For a dipolar dephasing CRAMPS experiment, $\pi/2$ and π pulses spaced by τ delays were added before BR-24 pulse train ($\pi/2-\tau-\pi-\tau-$BR-24). 2τ delay was incremented from 3 to 1000 μs.

Calculations. Chemical shift calculations and geometry optimizations were performed with the Gaussian 98 program package[32] using the DFT approach. Molecular geometries were completely optimized at the DFT level with the B3LYP functional,[33] the basis set being of 6-31G(d) quality. The gauge-including atomic orbitals (GIAO)[34,35] method was employed to calculate absolute shielding constants (σ, in ppm) for TMS and model structures. Subtraction gave the calculated chemical shifts (δ, in ppm) of the model structures relative to TMS. The basis set of 6-311+G(2d,p) quality was used in the computation of the ^{13}C NMR shifts.

Spin diffusion curves were calculated according to a strategy proposed by Schmidt-Rohr et al.[19,22] for the two-phase system with an interface and for variable dimensionality. The analytical solution starts for a simplified diffusion equation with spatially constant diffusivity with the solution of a finite source in an infinite surrounding. The derived equations are then used for a case with spatially variable diffusivity after replacing constant spin diffusion coefficient by effective diffusivity as described below in the section Domain Size and Morphology of the System.

Results and Discussion

DSC. The heats of fusion of PC and PEO in the blends are plotted in Figure 1 as functions of the weight fraction of PEO. For neat PC and PEO, the crystallinities of 20.8 and 85.5% were found, respectively, using the heats of fusion of fully crystalline polymers stated in the Experimental Section.

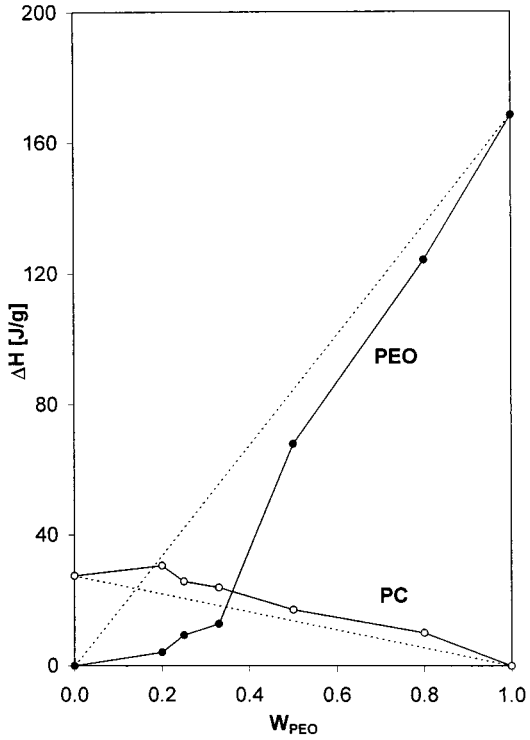

Figure 1. Dependence of heats of fusion of PC and PEO on the weight fraction of PEO in the PC−PEO blend.

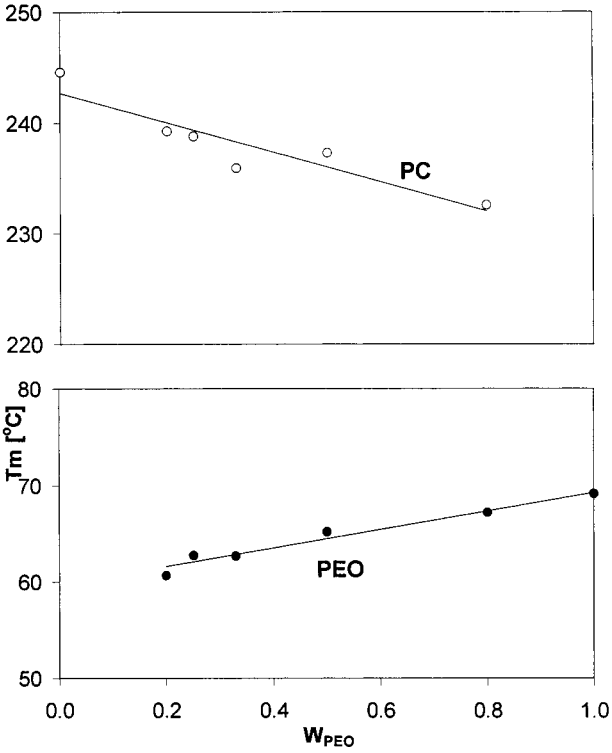

Figure 2. Dependence of melting temperatures of PC and PEO on the weight fraction of PEO in the PC−PEO blend.

The dependences of the heats of fusion of PC and PEO on the blend composition depicted in Figure 1 differ considerably. The values of PC show systematic positive deviations from the line corresponding to a linear decrease in the crystalline PC fraction with the decreasing PC content in the blend. This positive deviation implies a stimulating effect of the presence of PEO on crystallization of PC as described for one type of polymer pairs listed in the classification of blends of two semicrystalline polymers according to their mutual influence.[36] Such a stimulation is usually accounted by a decrease in glass transition temperature of the higher melting polymer in blends of two semicrystalline polymers miscible in the amorphous phase. A lower T_g leads to a higher mobility of polymer chains and an increased propensity of particular polymer to crystallize.[36,37] This is obviously the case of PC which, in the neat form, crystallizes relatively unwillingly. As can be seen from Figure 1, the crystallinity of PC in the blends is systematically higher than would correspond to the weight fraction of the neat polymer. A similar situation in the PC crystallization was found by Cheung at al. in the blends of PC with poly(ϵ-caprolactone), PCL.[38]

On the other hand, the crystallinity of PEO in the blends is substantially lower than that corresponding to the neat polymer. As shown in Figure 1, below the weight fraction of PEO 0.2, the crystallinity of PEO is almost negligible. According to the above-mentioned classification,[36] this behavior corresponds to the system where crystallization of one polymer is retarded or even partially prevented by the presence of the other polymer component in the blend. For a blend of two semicrystalline polymers, this phenomenon can be explained by the fact that at crystallization temperatures of the lower melting polymer, the higher melting one is already crystalline, and its structure hampers free growth of the other component crystals. Such behavior was found in blends of PC with PCL[38] and of poly(vinylidene fluoride) (PVF_2) with poly(butane-1,4-diyl adipate) (PBA).[37] In both cases, the two blended polymers were semicrystalline and miscible in the amorphous phase.

Miscibility of the PC−PEO blend in the amorphous phase, as suggested on the basis of spectroscopic measurements and determination of the heats of fusion, has also been corroborated by analysis of melting point depression. In Figure 2, one can see a steady decrease of the melting temperature of both PC and PEO with increasing concentration of the other polymer component. Such behavior is generally taken as a proof of partial miscibility of a given polymer pair in amorphous phase.

From the values in Figure 2 we have attempted to estimate the interaction parameter χ_{12} using a well-known procedure of Nishi and Wang.[39] We obtained the values −0.56 and −0.04 for parameter χ_{12} at the melting point of PEO and PC, respectively. However, the values should be considered as semiquantitative only as the measured values of T_m were used in the calculations, and no extrapolation to equilibrium melting temperatures was made. Such a procedure is, of course, thermodynamically incorrect,[40] but on the other hand, one should take into account that extrapolation to equilibrium conditions is generally associated with a great degree of uncertainty, and the resulting error in determining χ_{12} might be of the same order as that caused by using nonextrapolated T_m values.

The value of χ_{12} of approximately −0.5 suggests relatively strong interactions between PC and PEO in the amorphous phase and, consequently, at least partial miscibility in the amorphous phase at temperatures close to T_m of PEO, i.e., about 60 °C. On the other hand, the virtually zero value of χ_{12} at T_m of PC (about 240 °C) implies that the interaction parameter in the PC−PEO system is strongly temperature-dependent and that at T_m of PC the polymer pair obviously does not interact at all. One can contemplate that above T_m of

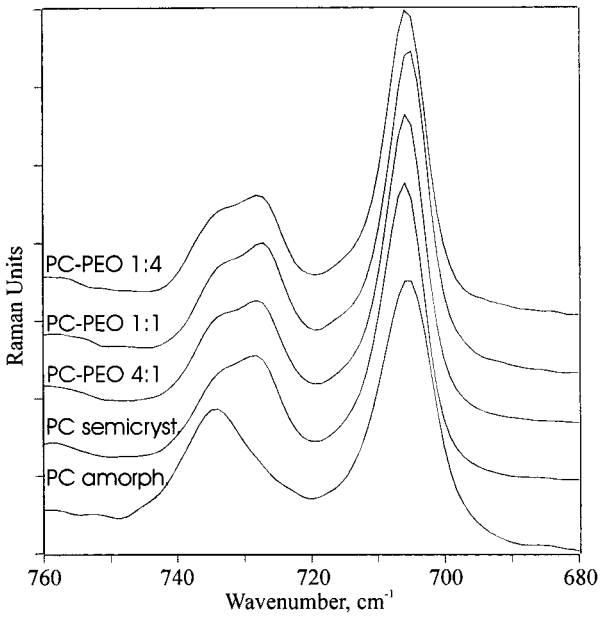

Figure 3. Raman spectra of amorphous and semicrystalline PC and the PC−PEO blends.

PC a low critical solution temperature might be expected in this system. However, no experiments in this respect have been carried out. In both the abovementioned systems of PC−PCL[38] and PVF_2−PBA,[37] the lower critical solution temperature was found at temperatures 50 and 70 °C above T_m of the respective higher melting polymer.

Raman Spectroscopy. Raman spectra of the original sample of amorphous PC together with the samples of PC and PC−PEO blends obtained by precipitation are shown in Figure 3. In comparison with the spectrum of amorphous PC, a new band at 728 cm^{-1} is detected in the spectra of semicrystalline PC and PC−PEO blends. This band was assigned to long regular-chain sequences in the crystalline phase of PC.[14] The intensity of the band at 728 cm^{-1} is slightly higher in the spectra of the PC−PEO blends compared with pure semicrystalline PC. Spectral subtraction performed in such way that no counterpeaks appear in the resulting spectrum[14] gives the values of 41% and 46% for the degrees of ordering of the PC chains in pure semicrystalline PC and in the PC−PEO 1−1 blend, respectively. This supports the results of the calorimetric measurements showing that the presence of PEO promotes the crystallization of PC in the PC−PEO blends.

^{13}C CP/MAS NMR Spectra. ^{13}C CP/MAS NMR spectra of neat PEO, amorphous, and semicrystalline PC as well as three PC−PEO blends are shown in Figure 4a−f. The signal assignment of PC (see Scheme 1) in ^{13}C CP/MAS NMR spectra was made on the basis of the results published in the literature.[8,10,11,16,41] Although the opposite signal assignment of signals 4 and 5 has been also published,[13] our experimental data (^{1}H−^{13}C dipolar dephasing experiment[42]) correspond to the former signal assignment. A bit faster ^{13}C magnetization decay of carbon with the signal at ca. 127 ppm indicates stronger effective heteronuclear ^{1}H−^{13}C dipolar interaction (see Figure 5). This interaction is slightly increased by neighboring, fast rotating methyl groups. The signal assignment generally accepted in the literature[8,10,11,16,41] and presented here is supported by ab initio calculations of the ^{13}C NMR chemical shifts for 4-$(CH_3)_3CC_6H_4OCOOCH_3$ (Figure 6) as an appropriate model compound for the chemical structure present in the PC chain. As reliable ab initio calculations of the chemical shifts require large basis sets, model compounds must be relatively small. In addition, these ab initio calculations well correspond to the empirical calculation of the ^{13}C NMR chemical shifts of the polycarbonate chain performed by using program package ADC/CNMR DB, Version 2.51. An interesting feature of these spectra is significant splitting of "low-field" signals corresponding to the carbon sites 3−7 in PC.

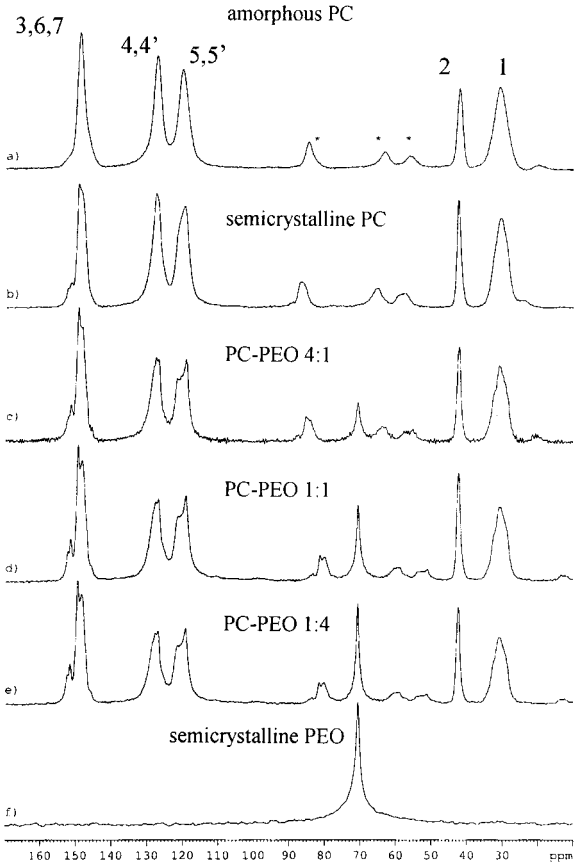

Figure 4. ^{13}C CP/MAS NMR spectra of amorphous PC (a), semicrystalline PC (b), blend PC−PEO 4−1 (c), blend PC−PEO 1:1 (d), blend PC−PEO 1:4 (e), and semicrystalline PEO (f). Mainly amorphous part of PEO is observed in these experiments. The small signals labeled with stars are spinning sidebands (SSB).

Scheme 1

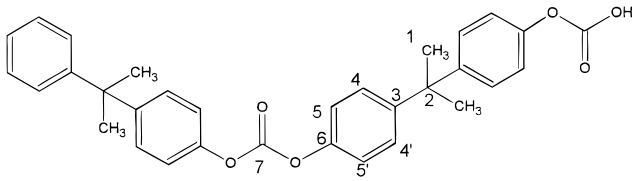

Recently published results of REDOR,[10] DRAMA,[12] CEDRA,[12] and DSR[12] experiments showed that glassy PC consists on average of densely packed chains. The determined short interchain ring−ring distance indicates that on a 10 Å scale the local orientation order is not completely random, and the proposed model for the glass has elements of crystalline-like packing.[9,10,12] However, also such packed materials show extensive mobility. PC motion mechanism involves 180° flips of phenyl rings at frequency 300 kHz (at room temperature) augmented by small-angle fluctuations of ±15°

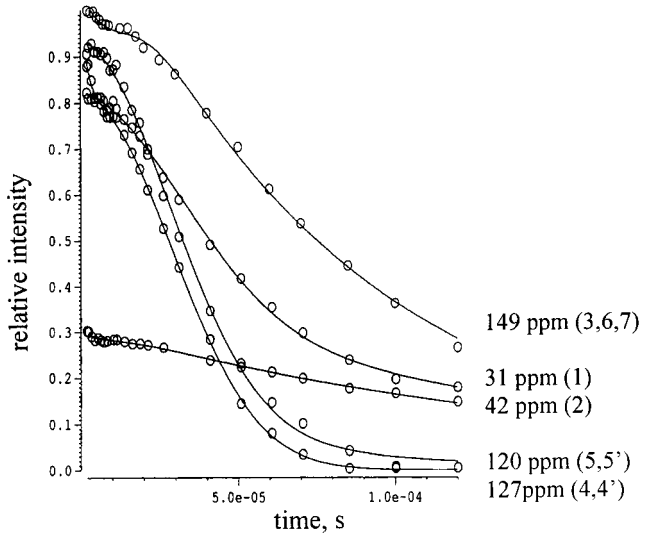

Figure 5. Heteronuclear $^1H-^{13}C$ dipolar dephasing of magnetization of pure amorphous PC detected through ^{13}C magnetization.

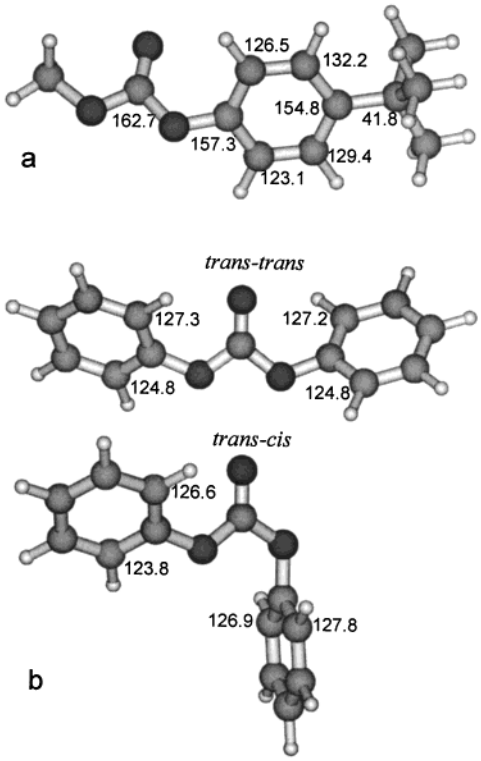

Figure 6. DFT-optimized (at the B3LYP/6-31G(d) level) structures of the model compound $(CH_3)_3C-(1,4\text{-}C_6H_4)-O-(CO)-O-CH_3$ (a) and trans−trans and trans−cis structures of diphenyl carbonate (b). ^{13}C NMR chemical shifts were calculated at the B3LYP/6-311+G(2d,p) level.

about the same C_2 axes. The overall spatial coordinate for this process is not the ring axes C_2 around which the flip occurs but rather a generalized spatial coordinate that also involves the positions of neighboring side groups and the main chain.[4,43] Proposed cooperative motions involve flipping of at least two rings down the chain and four or five other rings on other chains.[13,44] Such fast molecular motion easily averages out a possible chemical shift dispersion due to magnetic nonequivalence of the ^{13}C nuclei following from different orientation, packing, and conformation. That is why in completely amorphous neat PC only small asymmetry of the signal at ca. 149 ppm and no splitting of protonated aromatic carbon signals was observed. Asymmetry of the former line reflects inhomogeneous broadening, which is caused by overlapping of three probably homogeneously broadened signals of carbons 3, 6, and 7. The line shape of these three ^{13}C signals is given by variation of molecular packing and conformation nonequivalence and dynamic "homogeneous" broadening. In general, protonated aromatic carbons 5, 5′ (and 4, 4′) have nonequivalent local environment, because the aromatic rings are twisted with respect to the isopropylidene group so that the rings interact differently with the methyls and adjacent aromatic rings.[5,8] These signals, in particular those reflecting the 5,5′-positions, are also sensitive to different conformations of the carbonate group (trans−trans and trans−cis) as is demonstrated by ab initio calculations of the ^{13}C NMR chemical shifts for the model compound, diphenyl carbonate (Figure 6). Although the content of the trans−cis conformation (relative to trans−trans) was determined very low (less than 10% at room temperature),[45] our recently published results based on infrared and Raman spectra indicate substantially higher amount of the trans−cis conformations;[14] this is also supported by the model DFT calculations at the B3LYP/6-31G(d) level according to which the Gibbs energy difference between the trans−cis and trans−trans conformational states of diphenyl carbonate is only 0.9 kcal/mol.[14] We suggest that the changes observed in the ^{13}C CP/MAS NMR spectra of semicrystalline PC and PC−PEO blends in comparison with the spectrum of neat amorphous PC (see Figure 4a−f) indicate restricted mobility and hindered cooperative motions resulting from blending of PC with PEO and from fixed-chain ordering due to partial crystallinity of PC itself. As the crystallinity of PC determined by WAXS and DSC is relatively low (ca. 20%), molecular mobility is probably restricted not only in crystallites themselves but the presence of crystallites also retards cooperative motions in the neighboring amorphous phase.

It can be seen in Figure 4 that additional blending of PC with PEO causes an increase in splitting of the signals. The degree of crystallinity of PC is only slightly changed by blending with PEO and it is highly probable that dynamic behavior of PC molecules in crystallites is unaffected by the presence of PEO molecules in the blends. Thus, the observed splitting must be caused by slowing down of molecular motions of PC in the amorphous phase in the presence of PEO molecules, which indicates intimate mixing of PC with PEO almost at molecular level. We suggest that multiple splittings of the signal at ca. 120 ppm and weaker carbonate carbon signal at ca. 150 ppm also reflect the presence of two different conformations of the carbonate group (trans−trans and trans−cis). In addition to two nonequivalent carbon sites 5 and 5′ in the trans−trans structure of the diphenyl carbonate sequence (the orientation of the carbonate group is not perpendicular to the plane of aromatic rings; however, orientations of both phenyl rings are symmetric[14]), this signal must correspond as well to four nonequivalent sites in the trans−cis conformation (Figure 6). Although the above-mentioned splittings of the signals could be connected also with different chain packing, we suppose that differences in packing, disturbing electronic clouds of the carbons via variable short-range interactions,[14] have smaller effects than the orientations of phenyl rings with respect to the

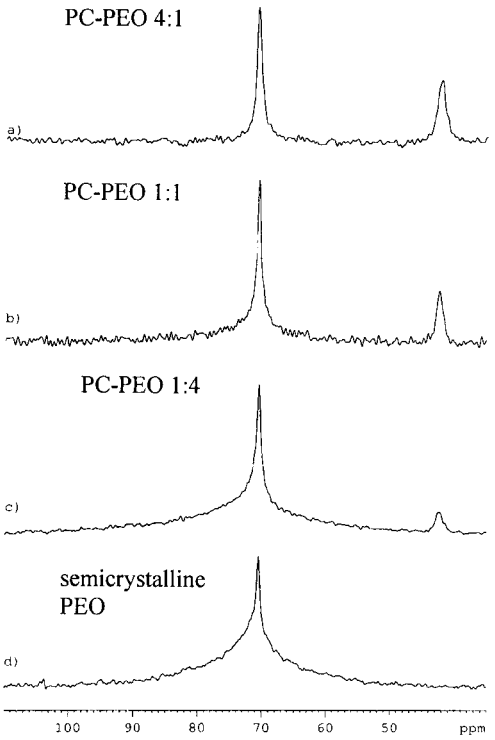

Figure 7. ^{13}C SP/MAS NMR spectra of the blends PC−PEO 4−1 (a), PC−PEO 1−1 (b), PC−PEO 1−4 (c), and semicrystalline PEO (d). Expanded region of the PEO signal. Amorphous and crystalline parts of PEO are detected.

carbonate carbon as the result of different conformations. The observed relative intensities of the components in the split signal indicate comparable amounts of both conformational structures, as was proposed on the basis of DFT calculations and Raman spectroscopy.[14] Further, we suggest that the weaker signal at 151.5 ppm can be attributed to the carbonate carbon, and although an unequivocal assignment cannot be performed on the basis of our results and calculations (see Figure 6), we assume that the resolved signals at 149.3 and 148.3 ppm correspond to nonprotonated aromatic carbons 6 and 3, respectively.

Differences in the line shape of the PEO signal in ^{13}C SP/MAS NMR spectra (SP = single pulse) of neat PEO and various PC−PEO blends (Figure 7) reflect changes in the degree of crystallinity and mobility of amorphous phase of PEO due to blending. The resonance of the crystalline phase is "downfield" shifted by about 1 ppm.[5,15] The crystalline peak obtained by deconvolution at ca. 72 ppm reflects a helical structure with a period of seven units in two turns and trans (COCC)−gauche (OCCO)−trans (CCOC) conformation for the repeat unit $-CH_2CH_2O-$.[15] However, due to destructive interference of motion of crystalline segments with dipolar decoupling, which is in this case ineffective, the line becomes homogeneously broadened.[5,46] The dynamic homogeneous broadening is observed when molecular motion produces C−H dipolar couplings fluctuating at a frequency close to the MAS and/or the angular frequency of the proton decoupling field. Higher decoupling field (at 80 kHz and higher) makes it possible to observe this broad resonance. Thus, MAS/DD line-width experiments can probe mid-kilohertz molecular mobility.[5] Moreover, the ^{1}H $T_{1\rho}$ and cross-polarization transport parameters in the crystalline and amorphous phases differ by 2 orders of magnitude in some temperature ranges.[47] Due to all these facts, the spectra for

Table 1. Line Width and Intensity of Crystalline, Interface, and Amorphous Components of PEO Determined by Deconvolution of the ^{13}C SP/MAS NMR Spectra and DSC and WAXS Crystallinities in PEO and PC−PEO Blends[a]

	NMR line width (Hz)			NMR intensity (%)			DSC (%)	WAXS (%)
polymer	a	i	c	a	i	c	c	c
PC− PEO 4−1	40			100			2	<14
PC− PEO 1−1	33	188	935	23	29	48	34	35
PC−PEO 1−4	24	178	1165	8	14	78	62	62
PEO	20	171	815	6	14	80	84	82

[a] Abbreviations: a = amorphous; i = interface (mesophase); c = crystalline.

quantitative evaluation have to be measured in a single-pulse experiment with repetition delay of 75 s, high-power proton decoupling field (80 kHz), and MAS frequency of 7 kHz to remove spinning sidebands from spectra (see Figure 7a−d). Deconvoluted line shapes and signal intensities of crystalline and amorphous PEO are listed in Table 1. Non-Lorentzian or super-Lorentzian line shape clearly indicates a substantial distribution of correlation times. Because of this fact, at least three Lorentzian components have to be used for the best fitting. Besides changes in relative intensities of the two PEO resonances reflecting changes in crystallinity of PEO, the widths are slightly affected by blending. This is striking for the amorphous PEO components (both two narrow lines; see Table 1): the line width (full width at half-intensity) were found to be always higher in blends compared with only 20 Hz in neat PEO. The origin of the spectral broadening may be a reduction in chain mobility for amorphous PEO caused by mixing with PC, resulting from an interaction between molecules of PC and PEO. Crystallinity of PEO decreases with increasing content of PC in a blend. This confirms intimate mixing of both components.

^{1}H NMR. As the present polymer systems are very complicated semicrystalline materials with motional heterogeneities, it is impossible to decompose the static ^{1}H spectra (not shown here) and to obtain information about specific motional processes. ^{1}H wide-line NMR spectra predominantly reflect immobile segments of PC as well as crystalline PEO as broad lines. Line widths of crystalline PEO and PC are 46 and 39 kHz, respectively. These lines are not affected by sample rotation at the rate of 3.2 kHz due to the fast magnetization decay occurring within the rotor period. On the other hand, MAS at 3.2 kHz additionally narrows the narrow line representing mobile component of PEO to line width ca. 170 Hz. This significant line narrowing and the presence of spinning sidebands reflect anisotropic motions with rates exceeding 1 MHz.

Dipolar dephasing rate is an important probe of the effective strength of the dipolar interactions. The standard Hahn-echo pulse sequence without or with slow MAS monitors dipolar dephasing caused by both coherent and incoherent processes. Under high-speed MAS and by application of the refocusing π pulse, which is synchronized with the rotor period, the coherent time evolution of the spin system can be inverted or produce an echo. (Note that the homogeneous part of homonuclear interactions of abundant spins—bilinear interactions in the spin system—cannot be refocused completely.) Thus, in the case of high-speed MAS with rates at least 18 kHz, we observe dipolar dephasing caused predominantly by the incoherent processes (relaxation),

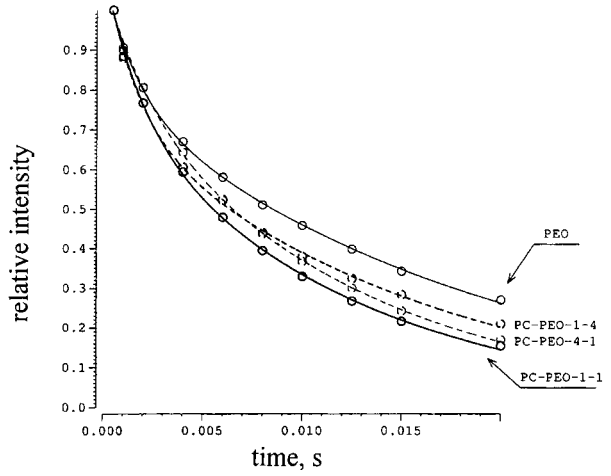

Figure 8. Homonuclear $^1H-^1H$ dipolar dephasing of magnetization of amorphous PEO detected through the ^1H magnetization measured at a high spinning speed 18 kHz.

because the coherent effects are more or less averaged out. The significant differences in the dipolar dephasing rates between various blends and single PEO are shown in Figure 8. The dephasing rate for abundant nuclei increases with decreasing molecular dynamics; in this way intensity of homonuclear dipolar interaction increases, and thus the magnetization decay during the dephasing period is speeded up. The dependences determined for the narrow signal of amorphous PEO at high spinning speed (18 kHz) reflect the strength of the fluctuating local magnetic fields. From determined dipolar dephasing rates it clearly follows that mobility of amorphous PEO is restricted in all polymer blends. As resolution of the ^1H MAS spectra is very low, we also used a sensitive and time-saving technique based on the combination of simple Hahn-echo experiment with multipulse averaging of dipolar interaction during data acquisition (CRAMPS). These spectra are well resolved (cf. Figure 9a) with distinguished three signals corresponding to aromatic (6.1 ppm) and methyl (1.7 ppm) protons of PC and methylene protons (4.3 ppm) of PEO. By this method, we compared dipolar dephasing rate of two blends PC−PEO 1−1 and PC−PEO 4−1. At first sight it is clear that molecular mobility of PC as well as PEO decreases with increasing content of PEO in the blend, which is reflected by faster magnetization decay of all three signals of the blend PC−PEO 1−1 (cf. Figure 9b−d).

2D WISE. A suitable NMR technique for investigation of the existence of mobility heterogeneities is 2D WISE spectroscopy. It allows obtaining a combination of structural and dynamic information. Differences in molecular mobility are probed by ^1H wide line shapes, which are separated in the second dimension by the ^{13}C chemical shift. High molecular mobility results in narrow ^1H lines and vice versa. To avoid spin diffusion during the spin lock pulse, it was set to 750 μs. The corresponding 2D WISE spectra as well as ^1H dipolar slices for amorphous PC and blend PC−PEO 4−1 are summarized in Figure 10. They show each chemically distinct ^{13}C resonance correlated with a ^1H powder pattern reflecting mobility. It has to be noted that predominantly only amorphous PEO is detected, as the crystalline part has a very short $T_{1\rho}(^1H)$ relaxation. Because of different mobility of the crystalline and amorphous phases of PEO, cross-polarization transport parameters and spin−lattice relaxation times in rotating frame may be very different. In general, for a creation of carbon magnetization in the crystalline part of PEO via cross-polarization, it is necessary to use very short spin-lock time (ca. 100−120 μs).[5,15] A spin-lock time of 750 μs used in our experiments is still very long. Because of fast $T_{1\rho}(^1H)$ relaxation of crystalline PEO, which is ca. 100 μs, carbon magnetization of crystalline PEO cannot be created and thus detected. It finally leads to a magnetization filter effect for the crystalline component of PEO.

In proton dipolar spectra there are some prominent features, which have to be pointed out. First, all signals corresponding to PC are significantly broader than the PEO signal. In all blends, we observe homogeneous line broadening of aromatic signals of PC with line width ca. 30 kHz, reflecting the presence of rigid segments on the 50 kHz time scale. In contrast, narrow line at 70 ppm attributed to the methylene carbon signal of amorphous PEO indicates mobility on the megahertz time scale. A very narrow line in the ^1H dimension corresponds to dipolar couplings almost averaged out by fast molecular motions, which are typical of amorphous polymers above glass transition temperature.[48] Huge differences in the proton dipolar line shapes observed in the spectra of PC−PEO blends confirm that no mobility of highly mobile amorphous PEO is imparted to PC in any significant portion.

Interesting information follows from the comparison of the ^1H dipolar spectra of aromatic signals of PC in blends and in neat amorphous PC (see Figure 10). Typical spinning sidebands are characteristic of ^1H dipolar spectra of aromatic signals of amorphous PC. These proton sidebands can be understood by considering that the intermolecular dipolar interactions are weakened by molecular motions, in particular rotations about a single axis, while the dipolar interactions of the phenyl protons along the flip axes are unchanged, and these relatively isolated proton pairs yield spectra with spinning sidebands.[21] No spinning sidebands are observed in proton dipolar spectra of all blends. This confirms restricted mobility and hindered cooperative motions resulting from blending of PC with PEO and from fixed ordering due to partial crystallinity of PC itself, following from ^{13}C CP/MAS NMR spectra.

Domain Size and Morphology of the System (^1H Spin Diffusion). To probe the extent of mixing of polymer blends PC−PEO, we first performed 2D exchange experiment exploiting ^1H spin diffusion with high-sensitivity ^1H detection using CRAMPS technique in both time evolution domains. As displayed in Figure 11, cross-peaks indicating proximity between aromatic and methyl protons of PC molecule are fully equilibrated after 150 μs. The first very weak cross-peaks were observed after 50 μs. This indicates the shortest interatomic distance between methyl and aromatic protons, ca. 0.3−0.4 nm, which is in accord with models of PC. In this way, we verified the validity of very simple formula for the maximum diffusive path length, $L = (6D_i\tau)^{1/2}$ where D_i is spin diffusion coefficient and τ is a delay time for spin diffusion process, which we used for the estimation of intermolecular distance between PC and PEO. The determination of the spin diffusion coefficient is described below. The first cross-signals indicating dipolar interaction between methylene protons of PEO and both-type protons of PC molecule are perceptible in 2D spectrum measured with 300 μs mixing time (PC−PEO 1−1). This indicates that the

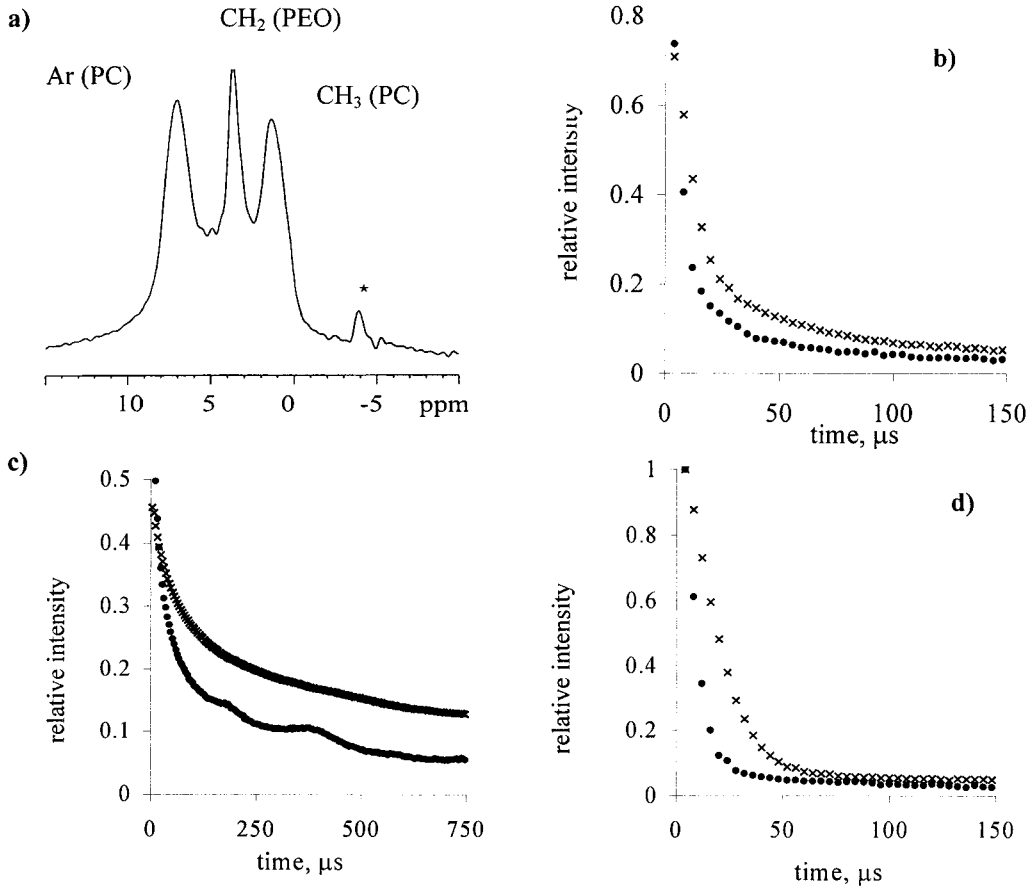

Figure 9. ^{1}H CRAMPS spectrum of the blend PC−PEO 1−1 (a). Homonuclear ^{1}H−^{1}H dipolar dephasing of the magnetization of PEO detected during homonuclear decoupling BR24. Magnetization decay of methylene protons of PEO (b), aromatic protons of PC (c), and methyl protons of PC (d). Dots (●) correspond to PC−PEO 1:1 and crosses (×) to PC−PEO 4:1.

smallest distance between PC and PEO is about 0.5−0.6 nm. However, even after 10 ms mixing time, the signals in 2D spectrum are not yet completely equilibrated, which means that in this material are heterogeneities larger than several nanometers. These heterogeneities with high probability correspond to crystallites of PEO and PC. However, for detailed determination of the domain size, especially in the amorphous phase where both components are mixed, we performed the 2D spin diffusion experiment proposed by Spiess et al.[21] This ^{1}H spin diffusion experiment with ^{13}C detection is based on the presence of proton species differing in mobility and thus in dipolar strength, which mutually communicate by means of dipolar couplings. The spin diffusion of ^{1}H magnetization is detected through the amplitude modulation of ^{13}C magnetization generated by cross-polarization. If a mixing time is permitted to allow spin diffusion during the WISE experiment, the motional narrowing associated with PEO proton lines can be transferred to the signals of PC carbons. Complete equilibration of ^{1}H magnetization is reflected in equal line shapes of all lines in proton wide-line dimension (cf. Figure 12).

The evaluation of spin diffusion curve was performed using a strategy proposed by Schmidt-Rohr et al.[19,22] for the two-phase system with an interface and for variable dimensionality, $\epsilon = 1-3$. The effective diffusivity, calculated according to the following equation

$$\sqrt{D_{\text{eff}}} = \frac{2r\sqrt{D_{\text{PEO}}D_{\text{PC}}}}{\sqrt{D_{\text{PEO}}} + r\sqrt{D_{\text{PC}}}} \qquad (1)$$

was used to simulate the spin diffusion process. The proton spin density ratio is defined as $r = \rho_{\text{PC}}/\rho_{\text{PEO}}$. The expression for the diffusivity in terms of local dipolar fields proposed by Cheung[49,50] was used for the determination of these coefficients, although other expressions relating diffusivity to T_2 relaxation were proposed.[7] However, the relation between diffusion coefficient and dipolar coupling, as reflected in the ^{1}H line width, is not quite clear[24,51] mainly because very narrow lines and simple scaling with the line width yields D values which are smaller than experimentally acceptable, indicating the influence of the $\langle r^2\rangle$ prefactor or other processes, such as diffusion of mobile segments in space. Diffusivity for amorphous PEO protons was calculated from the equation[26]

$$D_{\text{PEO}} = \frac{1}{6}\langle r^2\rangle[\alpha\Delta\nu_{1/2}]^{1/2} \qquad (2)$$

where $\langle r^2\rangle$ is the mean-square distance between the nearest spins (the average proton−proton separation in organic polymers is typically 0.2−0.25 nm[22,23]), α is the cutoff parameter, and $\Delta\nu_{1/2}$ is the full width at half-intensity for the Lorentzian line shape. Diffusion coefficient for PC was calculated from an equation, which is valid for the Gaussian line shape:[26]

$$D_{\text{PC}} = \frac{1}{12}\sqrt{\frac{\pi}{2\ln 2}}\langle r^2\rangle\Delta\nu_{1/2} \qquad (3)$$

Proton wide-line signals obtained by 2D WISE experiment of selected structure units (PEO: $-CH_2-$ signal

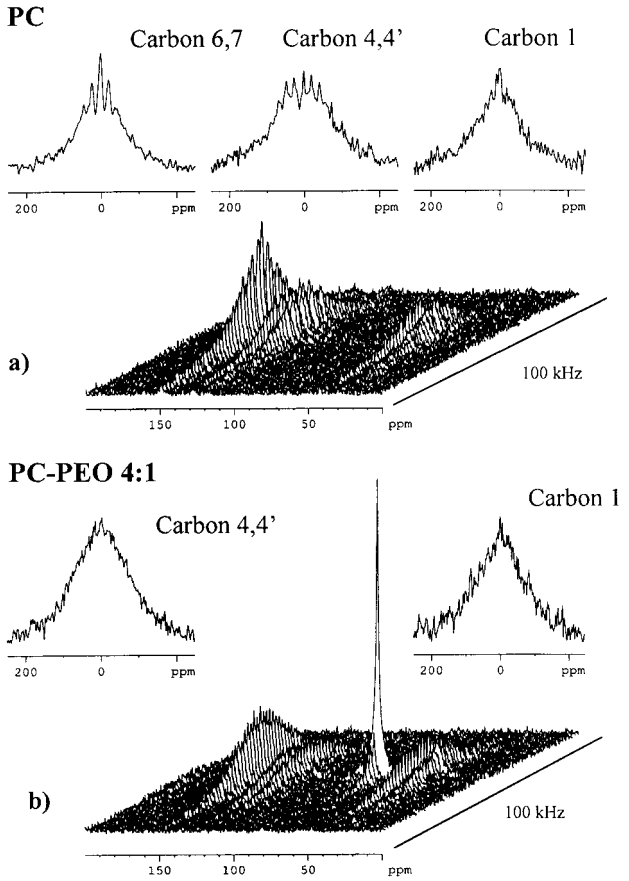

Figure 10. 2D WISE NMR spectra and ^{1}H dipolar slices of the PC sample (a) and the 4:1 PC−PEO blend (b).

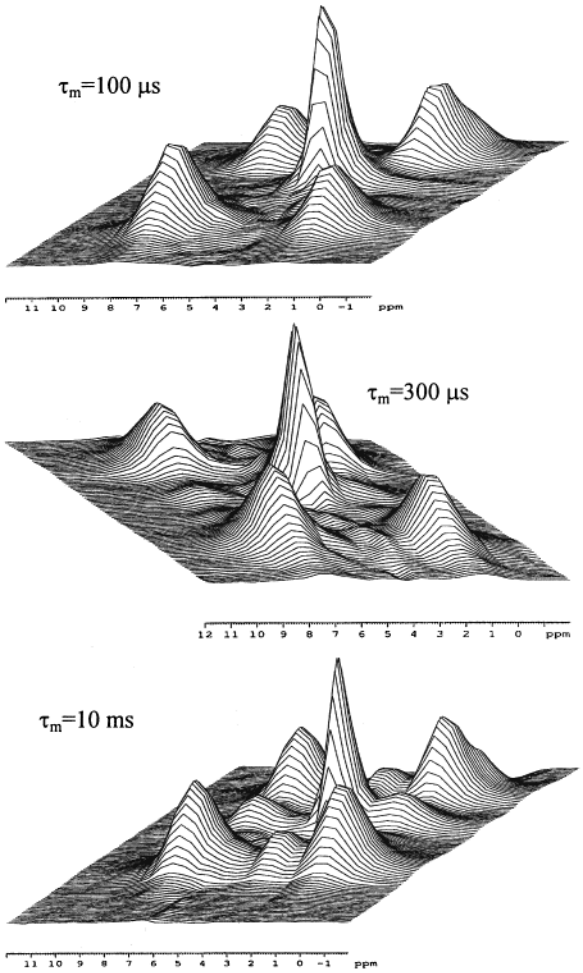

Figure 11. 2D ^{1}H exchange NMR spectra (CRAMPS, BR24) of the 1:1 PC−PEO blend measured at different mixing times τ_m.

at 72.5 ppm with half-width ca. 2.5 kHz; PC: aromatic −CH═ signal at 127.5 ppm with half-width ca. 40 kHz) were used to determine diffusivity. Line shapes of both signals are approximately the same for all samples. The calculated diffusivity for amorphous PEO is 0.11 nm^2 ms^{-1}, which is in good agreement with literature data.[26,52] Diffusivity of the PC segment has the value of 0.31 nm^2 ms^{-1}. In the literature,[48,53] spin diffusion coefficients are assumed to be 0.1 nm^2 ms^{-1} for mobile and 0.4 nm^2 ms^{-1} for rigid hard domains. Recent measurements of the spin diffusion coefficients from T_2 relaxation for mobile phases (amorphous PEO) reported by Mellinger et al.[54] (ca. 0.03−0.08 nm^2 ms^{-1}) are very close to our calculated values. Parameters that are necessary for analysis of the spin diffusion process are summarized in Table 2. In the first approximation, a two-component phase-separated system consisting of particles of amorphous PC domain on one side and amorphous PEO particles on the other side was taken into account.

Experimental and calculated data for all three PC−PEO blends are presented in Figure 13, which shows an increase in intensity of narrow component in originally broad proton dipolar spectra of the selected carbon (aromatic site 5) as a function of mixing time. Magnetization equilibrium is reached very quickly after ca. 15−20 ms indicating very small domain sizes. Linear extrapolation of the data in the region of very small values of $t^{1/2}$ does not pass through the time origin. This reveals the presence of an interface region between PC and PEO domains. Such an interface is connected to chain segments in the amorphous phase of PEO having restricted molecular motion. For the interfacial region, the spatially dependent spin diffusion coefficient was assumed to be varying linearly between the values of D_{PEO} and D_{PC}. However, the model for two-phase system with an interface is valid only for the 4:1 PC−PEO blend. In this blend, PEO is nearly completely amorphous and direct diffusion from the excited amorphous PEO phase into PC domains through the interface region can be considered. For the other blends with higher contents of PEO, we observe some deviation of magnetization behavior in the intermediate and late time regions of the spin diffusion process. This deviation is highly probably caused by the crystallinity of PEO. We assume that a part of PC is not dispersed in amorphous PEO, but it is located within interlamellar space of spherulites of PEO. The slowing down of the spin diffusion process is probably caused by the fact that magnetization from amorphous PEO has to transit into a part of PC through crystalline PEO lamellae, which is not directly excited by the used pulse sequence due to its rigidity. To analyze the spin diffusion curves for both blends with higher contents of PEO (1:1 and 1:4 PC−PEO), we modified numerical simulation of the spin diffusion so that simple single diffusion process was extended into the double spin diffusion process.

We propose that in the beginning the spin diffusion takes place only between PEO and PC in the amorphous phase. From this the domain sizes of both amorphous domains can be estimated. At longer times, spin diffusion occurs into crystalline PEO and the rest of PC.

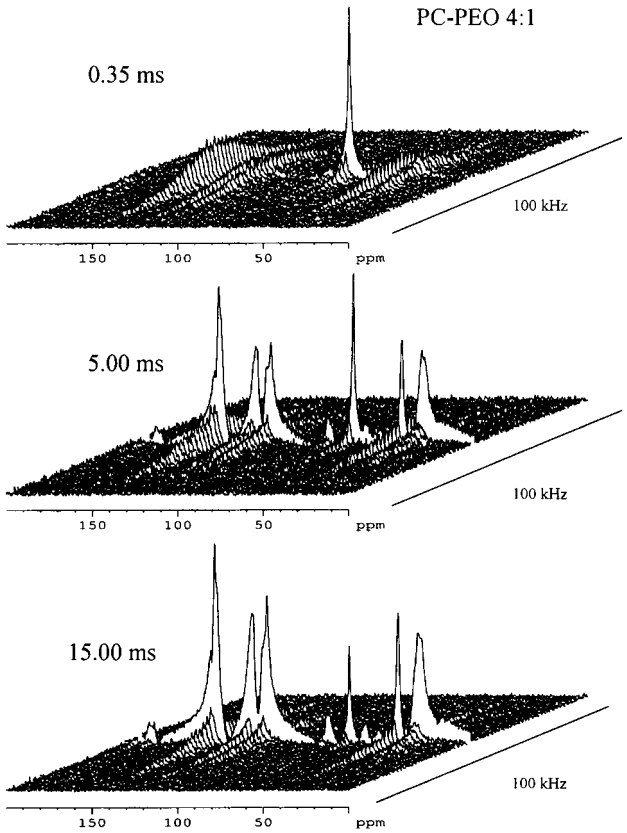

Figure 12. 2D WISE NMR spectra of the 4:1 PC−PEO blend measured with different mixing time for the spin diffusion.

Table 2. Calculated Diffusion Coefficients D_{PEO} and D_{PC}; Effective Diffusion Coefficient D_{eff}; Proton Fraction Φ; Density ρ_{PEO} and ρ_{PC} and Spin Density $\rho(s)_{PEO}$ and $\rho(s)_{PC}$

polymer	D,[a] nm^2 ms^{-1}	Φ	ρ, g cm^{-3}	ρ(s), g cm^{-3}
PEO	0.11	0.09	1.13	0.10
PC	0.31	0.05	1.14	0.06

[a] $D_{eff} = 0.21$ nm^2 ms^{-1}.

Therefore, we can conclude that in the 1:1 and 1:4 PC−PEO blends two spin diffusion processes are superimposed. The first process is the fast magnetization transfer from the most mobile amorphous PEO directly to adjacent PC. These two parts of the blends are in close spatial proximity. The second slow diffusion process starts in PEO itself by magnetization transfer from amorphous to crystalline PEO. However, this magnetization transfer cannot be detected in the spectra since crystalline PEO is undetected due to the interference of its molecular motions with the decoupling field. In the spin diffusion experimental data presented in Figure 13, it is manifested by a time delay, which is followed by a final transfer of magnetization from crystalline PEO to the part of PC located in the interlamellar regions of PEO. By using this model, experimental and calculated curves are in a good accord (see Figure 13). Unfortunately, we can only estimate the size of crystalline PEO domains, because we do not exactly know the fraction of crystalline PEO participating in this process. A generally accepted average value of crystallites in the literature is 7.1 nm [ref 26] or 19.6−21.3 nm [ref 52]. The calculated domain sizes, which are listed in Table 3, prove intimate mixing of PC and PEO in the amorphous phase. The results are divided into two main columns according to the spin diffusion process (fast, I; slow, II). The fast process is considered

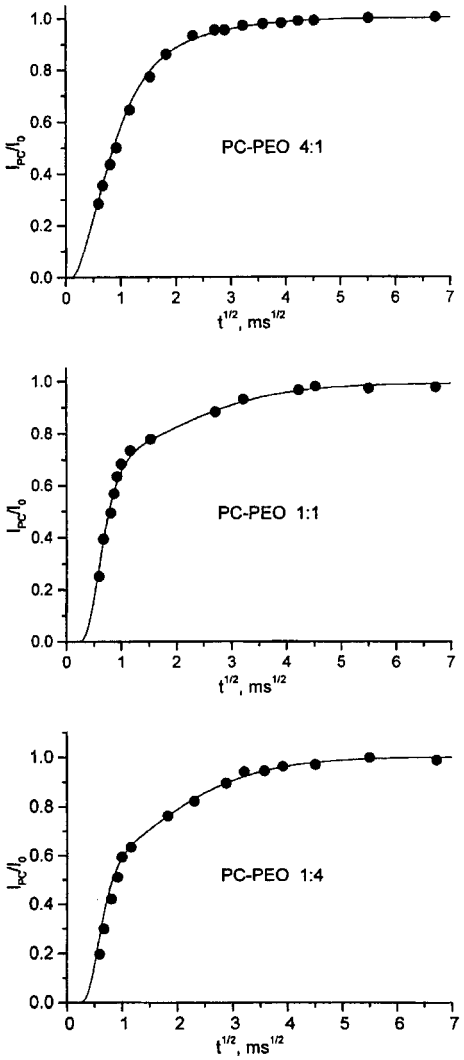

Figure 13. Experimental data and simulated spin diffusion curves of PC−PEO blends.

Table 3. Calculated Domain Sizes and Long Periods (nm) in PC−PEO Blends Obtained by Simulation of the Spin Diffusion Experiments

	fast process I				slow process II		
polymer	d_{PEO}	d_{PC}	$d_{interface}$	d_{long}	d_{PEO}	d_{PC}	d_{long}
PC−PEO 4−1	0.9	1.4	0.3	2.6	1.9	8.1	10.0
PC−PEO 1−1	0.3	0.4	0.7	1.4	3.9	3.9	7.8
PC−PEO 1−4	0.2	0.4	0.8	1.4	3.3	4.1	7.4

only between completely amorphous components (PEO and PC). For the second one, we also consider the presence of the crystalline part of PC (4:1 PC−PEO blend) and the presence of crystallites of PEO and part of PC placed between lamellae. This arrangement is confirmed by SAXS experiments (cf. Figure 14). The size of domains in the amorphous phase, which is smaller than 1 nm, directly proves mixing at the molecular level. Only a few molecules of one type of polymer form one or the other interface phase. This statement is confirmed by the determined dimensionality of this fast spin diffusion process (the best fit of the experimental data), which is in all cases two ($\epsilon = 2$). This two-dimensional process corresponds to the spin diffusion taking place from cylindrical or rodlike surface. Such process can be considered for one or several polymer chains of PEO aligned parallel. The interfacial region probably corresponds to immobilized PEO, which is in

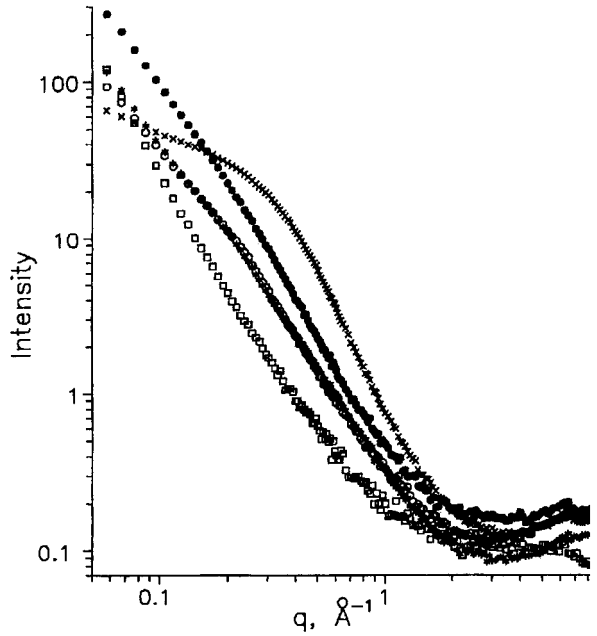

Figure 14. SAXS curves of PC (×), PEO (○), and blends PC−PEO 1−4 (∗), PC−PEO 1−1 (□), PC−PEO 2−1 (△), PC−PEO 3−1 (+), and PC−PEO 4−1 (●).

the closest environment of the PC chains. The determined size of the domains of crystalline lamellae of PEO and PC inside the spherulites is much larger (several nanometers) and is in accordance with the overall size of PEO crystallites. For this calculation, dimensionality of the process $\epsilon = 1$ was the best choice. SAXS measurements indicate that at least a part of the crystalline phase of PC is located inside the spherulites of PEO between the PEO lamellae (Figure 14). In comparison with pure PEO, no shoulder is detected in the SAXS diagram of the 1:1 PC−PEO blend. This is caused by low contrast in the PEO spherulites in the presence of PC in the blend, probably due to very close mass densities of crystalline PEO ($\rho_c = 1.28$ g/cm^3, $\rho_a = 1.125$ g/cm^3) and crystalline PC ($\rho_c = 1.31$ g/cm^3, $\rho_a = 1.20$ g/cm^3).[30] Incorporation of some PC chains into the amorphous interlayers of PEO can compensate density difference between crystalline lamellae and amorphous interlayers, resulting in suppression of the scattering effect on the lamellar structure.

Conclusions

Solid-state one-dimensional and two-dimensional ^{1}H and ^{13}C CP/MAS NMR spectroscopy was used to investigate the structure, morphology, and dynamic behavior of polymer blends based on PEO and PC. Splitting signals of aromatic carbons in ^{13}C CP/MAS NMR spectra and the absence of spinning sidebands in proton dipolar spectra (2D WISE) confirm restricted mobility and hindered cooperative motions of PC molecules resulting from blending of PC with PEO and from fixed ordering due to partial crystallinity of PC itself. Molecular mobility of PC is restricted not only to crystallites, but the presence of crystallites also retards the cooperative motions in neighboring amorphous phase (interface). Provided that line shape of the signals at ca. 150 and 120 ppm also reflects the presence of different conformations of the carbonate group, the observed multiple splitting of the signal indicates comparable amounts of the trans−trans and trans−cis conformational structures, which is in good accord with our ab initio calculations. Blending of PC with PEO also causes slowing down of the molecular motions of PEO in the amorphous phase, which was confirmed by the ^{13}C SP/MAS spectroscopy and ^{1}H−^{1}H homonuclear dipolar dephasing measurements. Blending also strongly decreases crystallinity of PEO and slightly increases crystallinity of PC. 2D WISE spectra confirm large differences in the molecular mobility of amorphous PEO and PC and the fact that no mobility of highly mobile amorphous PEO is imparted to PC in any significant portion. However, intimate mixing deduced from the ^{13}C CP/MAS NMR spectra and from ^{1}H−^{1}H homonuclear dipolar dephasing was proved by the spin diffusion measurements. The size of the domains in the amorphous phase is very small, below 1 nm. Larger regions with the size of several nanometers were found in the semicrystalline phase by spin diffusion and SAXS measurements. These regions correspond to PEO and PC lamellae inside the of PEO spherulites.

Acknowledgment. The authors thank the Grant Agency of the Czech Republic for financial support (Grant 203/97/0539). This work was partly sponsored by Grant LB98202 within the program INFRA2 of Ministry of Education, Youth and Sports of the Czech Republic (MSMT CR).

References and Notes

(1) Schmidt, P.; Dybal, J.; Straka, J.; Schneider, B. *Makromol. Chem.* **1993**, *194*, 1757.
(2) Straka, J.; Schmidt, P.; Dybal, J.; Schneider, B.; Spěváček J. *Polymer* **1995**, *36*, 1147.
(3) Schmidt, P.; Straka, J.; Dybal, J.; Schneider, B.; Doskočilová, D.; Puffr, R. *Polymer* **1995**, *36*, 4011.
(4) Schaefer, J.; Stejskal, E. O.; Perchak, D.; Skolnick, J.; Yaris, R. *Macromolecules* **1985**, *18*, 368.
(5) VanderHart, D. L.; Earl, W. L.; Garroway, A. N. *J. Magn. Reson.* **1981**, *44*, 361.
(6) Matsumoto, A.; Egama, Y.; Matsumoto, T.; Horii, F. *Polym. Adv. Technol.* **1997**, *8*, 250.
(7) Schantz, S.; Maunu, S. L. *Macromolecules* **1994**, *24*, 6915.
(8) Henrichs, P. M.; Nicely, V. A. *Macromolecules* **1990**, *23*, 3193.
(9) Lee, P. L.; Kowalewski, T.; Poliks, M. D.; Schaefer, J. *Macromolecules* **1995**, *28*, 2476.
(10) Schmidt, A.; Kowalewski, T.; Schaefer, J. *Macromolecules* **1993**, *26*, 1729.
(11) Goetz, J. M.; Wu, J.; Yee, A. F.; Schaefer, J. *Macromolecules* **1998**, *31*, 3016.
(12) Klug, C. A.; Zhu, W.; Tasaki, W.; Schaefer, J. *Macromolecules* **1997**, *30*, 1734.
(13) Horii, F.; Beppu, T.; Takaesu, N.; Ishida, M. *Magn. Reson. Chem.* **1994**, *32*, S30.
(14) Dybal, J.; Schmidt, P.; Baldrian, J.; Kratochvíl, J. *Macromolecules* **1998**, *31*, 6611.
(15) Schantz, S. *Macromolecules* **1997**, *30*, 1419.
(16) Wei, K.; Ho, J. *Macromolecules* **1997**, *30*, 1587.
(17) Mirau, P. A.; White, J. L. *Magn. Reson. Chem.* **1994**, *32*, S23.
(18) Caravatti, P.; Neuenschwander, P.; Ernst, R. R. *Macromolecules* **1986**, *19*, 1889.
(19) Schmidt-Rohr, K.; Spiess, H. W. *Multidimensional Solid-State NMR and Polymers*; Academic Press: New York, 1994.
(20) Zumbulyadis, N. *Phys. Rev. B* **1986**, *33*, 6495.
(21) Schmidt-Rohr, K.; Clauss, J.; Spiess, H. W. *Macromolecules* **1992**, *25*, 3273.
(22) Clauss, J.; Schmidt-Rohr, K.; Spiess, H. W. *Acta Polym.* **1993**, *44*, 1.
(23) Chin, Y. H.; Kaplan, S. *Magn. Reson. Chem.* **1994**, S*53*, 32.
(24) Cai, W. Z.; Schmidt-Rohr, K.; Egger, N.; Gerhartz, B.; Spiess, H. W. *Polymer* **1993**, *34*, 267.
(25) Quijada-Garrido, I.; Wilhelm, M.; Spiess, H. W.; Barrales-Rienda, J. M. *Macromol. Chem. Phys.* **1998**, *199*, 985.
(26) Demco, D. E.; Johanson, A.; Tegenfeldt, J. *Solid State Nucl. Magn. Reson.* **1995**, *4*, 13.
(27) Zhang, X.; Takegoshi, K.; Hikichi, K. *Macromolecules* **1991**, *24*, 5756.

(28) Lehmann, S. A.; Meltzer, A. D.; Spiess, H. W. *J. Polym. Sci., Part B: Polym. Phys.* **1998**, *36*, 693.
(29) Bin Yan, Stark, R. E. *Macromolecules* **1998**, *31*, 2600.
(30) Van Krevelen, D. W. *Properties of Polymers*, 3rd ed., Elesevier: London, 1990.
(31) Pines, A.; Gibby, M. G.; Waugh, J. S. *J. Chem. Phys.* **1973**, *70*, 3300.
(32) Frisch, M. J.; Trucks, G. W.; Schlegel, H. B.; Scuseria, G. E.; Robb, M. A.; Cheeseman, J. R.; Zakrzewski, V. G.; Montgomery, J. A., Jr.; Stratmann, R. E.; Burant, J. C.; Dapprich, S.; Millam, J. M.; Daniels, A. D.; Kudin, K. N.; Strain, M. C.; Farkas, O.; Tomasi, J.; Barone, V.; Cossi, M.; Cammi, R.; Mennucci, B.; Pomelli, C.; Adamo, C.; Clifford, S.; Ochterski, J.; Petersson, G. A.; Ayala, P. Y.; Cui, Q.; Morokuma, K.; Malick, D. K.; Rabuck, A. D.; Raghavachari, K.; Foresman, J. B.; Cioslowski, J.; Ortiz, J. V.; Stefanov, B. B.; Liu, G.; Liashenko, A.; Piskorz, P.; Komaromi, I.; Gomperts, R.; Martin, R. L.; Fox, D. J.; Keith, T.; Al-Laham, M. A.; Peng, C. Y.; Nanayakkara, A.; Gonzalez, C.; Challacombe, M.; Gill, B.; Johnson, P. M. W.; Chen, W.; Wong, M. W.; Andres, J. L.; Gonzalez, C.; Head-Gordon, M.; Replogle, E. S.; Pople, J. A. *Gaussian 98, Revision A.6*; Gaussian, Inc.: Pittsburgh, PA, 1998.
(33) Becke, A. D. *J. Chem. Phys.* **1993**, *98*, 5648.
(34) Ditchfield, R. *Mol. Phys.* **1974**, *27*, 789.
(35) Cheeseman, J. R.; Trucks, G. W.; Keith, T. A.; Frisch, M. J. *J. Chem. Phys.* **1996**, *104*, 5497.
(36) Utracki, L. A. *Polymer Alloys and Blends*, Hanser Publishers: Munich, 1990.
(37) Penning, J. P.; St. John Manley, R. *Macromolecules* **1996**, *29*, 77.
(38) Cheung, Y. W.; Stein, R. S. *Macromolecules* **1994**, *27*, 2512.
(39) Nishi, T.; Wang, T. T. *Macromolecules* **1975**, *8*, 909.
(40) Runt, J.; Gallagher, K. P. *Polym. Commun.* **1991**, *32*, 180.
(41) Klug, C. A.; Wu, J.; Xiao, C.; Yee, A. F.; Schaefer, J. *Macromolecules* **1997**, *30*, 6302.
(42) Alemany, L. B.; Grant, D. M.; Alger, T. D.; Pugmire, R. J. *J. Am. Chem. Soc.* **1983**, *105*, 6697.
(43) Spiess, H. W. *Colloid. Polym. Sci.* **1983**, *261*, 193.
(44) Romisszowski, P.; Yaris, R. *J. Chem. Phys.* **1991**, *94*, 6751.
(45) Tomaselli, M.; Zehnder, M. M.; Robyr, P.; Grob-Pisano, C.; Ernst, R. R.; Suter, U. W. *Macromolecules* **1997**, *30*, 3579.
(46) Stejskal, E. O.; Schaefer, J.; Sefcik, M. D.; McKay, R. A. *Macromolecules* **1981**, *14*, 275.
(47) Johanson, A.; Tegenfeldt, J. *Macromolecules* **1992**, *25*, 4712.
(48) Clauss, J.; Schmidt-Rohr, K.; Adam, A.; Boeffel, C.; Spiess, H. W. *Macromolecules* **1992**, *25*, 5203.
(49) Cheung, T. T. P. *Phys. Rev.* **1981**, *B23*, 1404.
(50) Cheung, T. T. P.; Gerstein, B. C. *J. Appl. Phys.* **1981**, *52*, 5517.
(51) Spiegel, S.; Schmidt-Rohr, K.; Spiess, H. W. *Polymer* **1993**, *34*, 4566.
(52) Weigand, F.; Demco, D. E.; Blümich, B.; Spiess, H. W. *J. Magn. Reson., Ser. A* **1996**, *120*, 190.
(53) Clayden, N. J.; Nijs, C. L.; Eeckhaut, G. J. *Polymer* **1997**, *38*, 1011.
(54) Mellinger, F.; Wilhelm, M.; Spiess, H. W. *Macromolecules* **1999**, *32*, 4686.

MA000533S